

Simulation of an Active Controlled Vibration Isolation System for Astronaut's Exercise Platform

Shield B. Lin, Sameer Abdali

Abstract—Computer simulations were performed using MATLAB/Simulink for a vibration isolation system for astronaut's exercise platform. Simulation parameters initially were based on an on-going experiment in a laboratory at NASA Johnson Space Center. The authors expanded later simulations to include other parameters. A discrete proportional-integral-derivative controller with a low-pass filter commanding a linear actuator served as the active control unit to push and pull a counterweight in balancing the disturbance forces. A spring-damper device is used as an optional passive control unit. Simulation results indicated such design could achieve near complete vibration isolation with small displacements of the exercise platform.

Keywords—Control, counterweight, isolation, vibration.

I. INTRODUCTION

HAVING sufficient exercise is extremely important to an astronaut's health during long flight missions [1], [2]. Exercise activities inevitably produce excited forces that generally are transmitted to the spacecraft and cause operation difficulty. In order to minimize the transmitted forces, the use of vibration isolation systems has been studied in a microgravity environment [3], [4]. NASA is in the process of designing, analyzing, and evaluating new countermeasures in vibration isolation systems. NASA needs to understand how the dynamic forces caused by operational countermeasures impact the spacecraft. The authors propose to use an active proportional-integral-derivative (PID) controller to direct the motion of a counterweight [5]-[8]. The authors also propose to add a passive control scheme to further regulate the movement of the exercise platform. The goals are to minimize the forces to be transmitted to spacecraft from exercising activities while to allow small and smooth movement of the exercise platform so that the exercisers feel comfortable using it.

II. EXPERIMENTAL SET-UP

As shown in Fig. 1, a prototype model of a one-dimensional Vibration Isolation System (VIS) is built in a laboratory at NASA Johnson Space Center. The prototype features a central control module flanked by two equal counter masses connected through separate mechanisms. One mass is connected via a spring while the other is connected through a linear actuator. The purpose of such a system is to offset any force in one dimension through both the spring and controlled

actuation. The entire assembly is placed on top of a single track to reduce as much friction as possible while constraining the VIS into one dimension. The control algorithm is run by an Arduino Uno with an MegaMoto Plus microcontroller. Position, velocity, and acceleration are determined through two laser rangefinders that point to a static location. One reads the actuator position and reads from a position fixed relative to the VIS motion. The other reads the central platform position and reads from an independently fixed position.

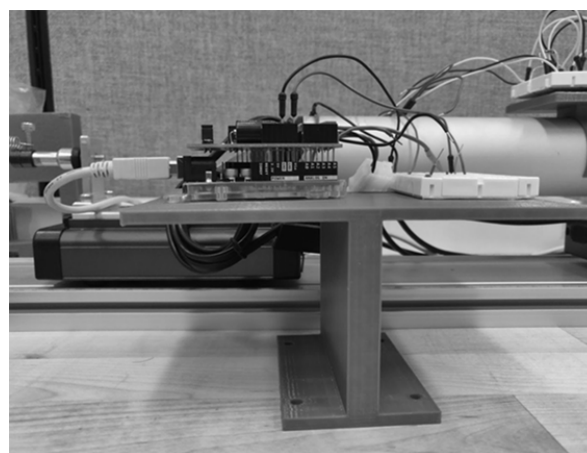


Fig. 1 One-Dimensional VIS Prototype in a Laboratory at NASA Johnson Space Center, Houston, Texas

The need for this prototype stems from a desire to test an overarching control algorithm on a smaller scale to reduce danger in case of any malfunction. Since the mass associated with this VIS is less than 6 kg in total, the risk of injury if the actuator is given a voltage which causes the mass to move unexpectedly is much lower than another assembly using mass in excess of 100 kilograms. Moreover, the design is meant to be modular and made of 3D printed parts, allowing for quick alterations to further test various components. An example of this is the current laser rangefinder assembly utilized in this build. The original design incorporated a series of sonar sensors in which the fidelity was far too low for any practical application. The prototype VIS allowed the team to discover the problem and initiated the resulting purchase of a higher resolution rangefinder. Additionally, this VIS is critical for modeling on more complex systems as much of the characterization of the equipment is conducted through this. Error, fidelity, resolution, and more are characterized and used in the simulation of more complex systems.

S. B. Lin is with the Department of Mechanical Engineering at Prairie View A&M University, Prairie View, Texas 77446 USA (corresponding author, phone: 936-261-9958; e-mail: shlin@pvamu.edu).

S. Abdali is with the Department of Mechanical Engineering at Prairie View A&M University, Prairie View, Texas 77446 USA (e-mail: sabdali@student.pvamu.edu).

III. MODELING OF VIS

The scenario of applying active control for a VIS can be illustrated as a mother, standing on an icy surface, who holds an active baby in one arm and a counterweight in another; she tries to move the counterweight to balance the excited forces from the active baby so that her feet can stand still on the frictionless surface. If adding a passive control unit to the illustration, one can consider it as tying a strut, i.e. a spring-damper device, at the mother's waist to a nearby fixed structure. The goal is to use the counterweight to maintain the force balance and to minimize the force to be transmitted through the strut to the structure. For complete vibration isolation, there will be no force being transmitted through the strut. The strut is just a safety feature in this case.

The authors have derived a one-dimensional active control

vibration isolation model. The one-dimensional system can be readily extended to two or three-dimensions if the VIS is designed to decouple the excited forces in multiple dimensions. A schematic diagram of the feedback control system is illustrated in Fig. 2. A PID controller and an Actuator serves as the active control unit to drive the exercise platform which receives disturbance input force from a human exerciser. The platform is also attached to a passive control unit which includes spring and damper components for reducing platform vibrations. Two major outputs of the system are displacement of platform and the force being transmitted to the wall, namely, spacecraft structure. A position sensor captures the platform displacement, x , and compare it to a reference signal, x_{ra} . The difference of the two values serves as the input to the PID controller.

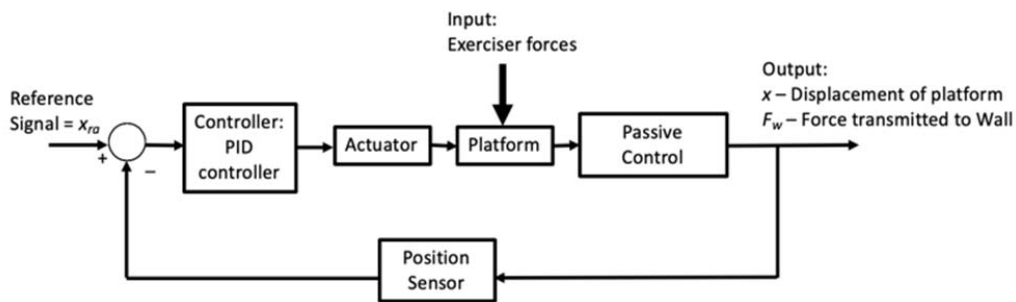


Fig. 2 Schematic Diagram of Feedback Control System for Vibration Isolation

A. Exercise Platform

The dynamics of exercise platform motion is directly governed by the Newton's 2nd Law. The total force applied to the platform, F_t , divides by the total mass attached to the platform, M_t , would be the acceleration of the platform, a . The total mass of the system includes human exerciser, platform, actuator, and counterweight. If applying active control only, the total force would be the excited force created by the exerciser plus the linear actuator force commanded by the active control unit. If applying both active and passive control, the total force would be the addition of damping force and spring force to the excited force, and actuator force. Acceleration of the platform, a , can be calculated by:

$$\sum F_t = M_t a \quad (1)$$

Platform velocity, v , and displacement, x , can be calculated by the following integrations:

$$v = \int a \, dt \quad (2)$$

$$x = \int v \, dt \quad (3)$$

B. Active Control Unit

A discrete PID controller commanding a linear actuator is used in the simulation to provide forces to push or pull a counterweight in the efforts to reduce or eliminate the effect causing by the exciter's forces. The PID controller takes an input signal, the difference between sensor feedback value and

a reference value, and provides an output signal. The output is a weighted sum of the input signal, the integral of the input signal, and the derivative of the input signal. The weights are the proportional, P , integral, I , and derivative, D , gain parameters. In order to reduce the noise in the input signal, a low pass filter with filter constant, N , is added to the derivative action. T_s is the sampling time for the controller.

Considering the physical limitation of the DC motor, a saturation function is incorporated in the PID control algorithm. At times, the calculated output from the controller is physically impossible, it is called integral windup which accumulates excessive high output by the control algorithm. In this case, saturation function provides anti-windup and turns off for periods of time until the response falls back into an acceptable range. This usually occurs when the controller's output can no longer affect the controlled variable [9]. The PID controller block and saturation function are illustrated in the block diagram in Fig. 3.

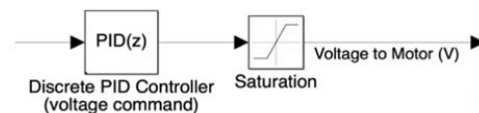


Fig. 3 Command Signals of Discrete PID controller Regulated by a Saturation Function

The discrete PID controller equation can be expressed as in (4):

$$PID(z) = P + I * T_s \frac{1}{z-1} + D * \frac{N}{1+N*T_s \frac{1}{z-1}} \quad (4)$$

The linear actuator has a DC motor which receives voltage commands from the controller. The rotor armature of the DC motor rotates under the action of a magnetic field produced by the electrical circuit of the stator. We assume that the magnetic circuit is linear and the mechanical friction is linear in the motor speed, the basic equations of a DC motor can be modeled by an electrical circuit equation and a mechanical torque equation. The circuit equation is governed by Kirchhoff's second law involving armature inductance, L_a , resistance, R_a , back electromotive constant, K_b , current, $i_a(t)$, voltage, $v_a(t)$, and angular velocity, $\omega(t)$.

$$L_a \frac{di_a(t)}{dt} + R_a i_a(t) = v_a(t) - K_b \omega(t) \quad (5)$$

Torque is developed due to the stator-rotor interaction that couples the mechanical and electrical fields. The torque, on mechanical side, is represented by the product of the mass

moment of inertia, J_l , and the angular acceleration, $d\omega(t)/dt$. Note that J_l should include the mass moment of inertia of the rotor in the DC motor as well as the equivalent mass moment of inertia of the counterweight through the lead screw. On the electrical side, torque is represented by the product of the motor constant, K_m , and the current, $i_a(t)$.

$$J_l \frac{d\omega(t)}{dt} = K_m i_a(t) \quad (6)$$

We divide (5) by L_a and rearrange its order to obtain:

$$\frac{di_a(t)}{dt} = \left(\frac{1}{L_a}\right) v_a(t) - \left(\frac{R_a}{L_a}\right) i_a(t) - \left(\frac{K_b}{L_a}\right) \omega(t) \quad (7)$$

where $\omega(t)$ can be obtained by integrating (6):

$$\omega(t) = \int \left(\frac{K_m}{J_l}\right) i_a(t) \quad (8)$$

Equations (7) and (8) can be represented by the DC motor block diagram in Fig. 4.

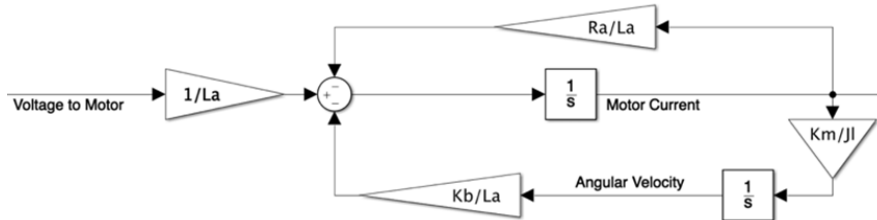


Fig. 4 DC Motor Block Diagram

The linear actuator force, $F(t)$, is generally proportional to the current, $i_a(t)$, of the DC motor, and can be calculated by 2π , i.e. 6.28, multiplying to the current and motor constant, K_m , and divided by the lead screw pitch, L .

$$F(t) = \left(\frac{2\pi K_m}{L}\right) i_a(t) \quad (9)$$

Due to friction effect, the absolute value of calculated actuator force must exceed certain thresholds to conquer the static friction and to drive the leadscrew to push or pull the counterweight. Hence, a dead zone dynamic function is added to the actuator force before it is applied to the counterweight on the exercise platform. The block diagram of the linear actuator force is illustrated in Fig. 5.

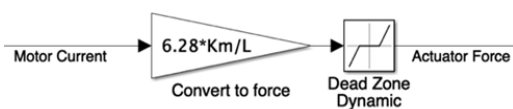


Fig. 5 Linear Actuator Force Block Diagram

C. Passive Control Unit

A spring and damper device is used as a passive control unit to damp down the forces being transmitted to spacecraft structure and to reduce the oscillation of the platform. Two applied forces are human force excited by the exerciser and actuator force from the active control unit. Two passive forces,

spring force is calculated by the product of a spring constant, K , and the platform displacement, x . Damping force is calculated by the product of a damper coefficient, C , and the platform velocity, \dot{x} . As described in the section of Exercise Platform, the total mass, M_t , is the sum of masses from the human exerciser, the exercise platform, actuator components, and the counterweight. The schematic diagram and equation of the passive control unit are shown in Fig. 6 and (10).

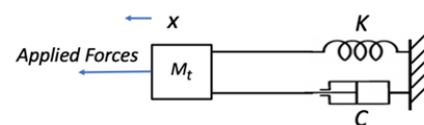


Fig. 6 Schematic Diagram of Passive Control Unit

$$M_t \ddot{x} + C \dot{x} + Kx = \text{Applied Forces} \quad (10)$$

Applied forces include human force and actuator force; the equation can be rewritten as:

$$\ddot{x} = \left(\frac{1}{M_t}\right) (\text{Human force} + \text{Actuator force} - C\dot{x} - Kx) \quad (11)$$

and the block diagram of the passive control unit is displayed in Fig. 7.

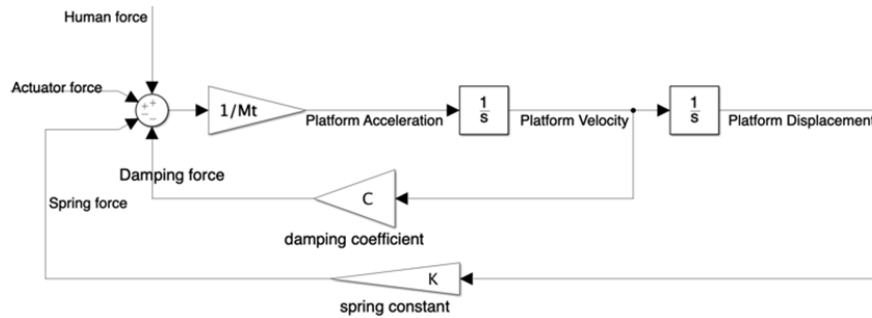


Fig. 7 Block Diagram of Passive Control Unit

IV. SIMULATION PARAMETERS AND PROCESS

Exciter forces for the real system are the forces when astronauts are doing exercises on the platform. For computer simulation, the exciter forces are scaled down to match the prototype experiment set-up in the lab at Johnson Space Center. MATLAB [10] is used to generate CSV files which represent a variety of exciter forces; and these files are placed in the input force block to the simulations in Simulink.

The primary simulation goal is to achieve vibration isolation, i.e., to minimize or even eliminate the forces transmitted to the structure of a spacecraft. The secondary goal is to ensure that astronauts feel comfortable when they perform exercise activities on the VIS platform. Feeling comfortable is subjective; the authors considered “comfortable” when dynamic responses of amplitude and frequency of the platform are both small. Exercisers may still feel comfortable with large platform amplitude when frequency is low. However, the available space for an exercise station is limited in a spacecraft; a large displacement of the exercise platform is not practical.

The simulation problem consists of three sets of differential equations: platform dynamic equations, motor-linear actuator equations and spring-damper equations; a difference equation, discrete PID controller with a low-pass filter for derivative control; and three constraints: saturation of DC motor capacity, dead-zone dynamic for linear actuator force, and feedback frequency of position sensor at the platform. There are six adjustable parameters for the system: three controller gains, P, I, D, filter constant N, spring constant K, and damping coefficient C. It is almost impossible to find a set of unique solutions of the six parameters that would lead to the “best” system, provided the “best” system cannot be precisely defined mathematically.

Simulink is used to build the model and to search for an optimal combination of the six adjustable parameters. A tuning algorithm on Simulink for the discrete PID controller is applied by selecting the scale of response time and transient behavior to obtain “suitable” control gains and derivative filter constant. “Suitable” gains and filter constant would diminish forces being transmitted to the “fixed” structure while maintaining small amplitudes and frequencies of platform movement. At times, these two goals conflict with each other and must be compromised.

Two major output parameters of the simulation are (1) force

transmitted to wall, i.e. “fixed structure” and (2) platform displacement. In the beginning of the simulation, the authors chose a combination of spring constant and damping coefficient as a set. Within this set, the authors used the tuning algorithm to adjust the combination of PID controller gains and the filter constant. For each simulation, the authors recorded the difference between the largest positive force (high peak) being transmitted to the wall and the largest negative force (low peak) being transmitted to the wall. For a set of simulations, the authors identified the one with the smallest peak-to-peak transmitted force as the “best”. The authors then inspected the platform displacement and frequency to decide if they were considered “comfortable”. If the answer was yes, the authors would record the set of six adjustable parameters along with the output as an acceptable simulation.

If the platform amplitudes and frequencies were large and considered not comfortable for astronauts’ exercise activities, the authors would perform fine adjustment to the control parameters. The goal of fine adjustment was to not deviate the acceptable transmitted force too much while reducing platform displacement and frequency to an acceptable level. If the fine adjustment goal was achieved, the authors would record the set of six adjustable parameters along with the output as an acceptable simulation. When completing a set of simulation, the authors moved to another pair of combination of spring constant and damping coefficient, and repeated the same process of tuning PID controller gains and the filter constant.

V. EXAMPLES OF SIMULATION RESULTS

An example of an acceptable simulation is shown in Fig. 8 with “100%” vibration isolation. The authors set spring constant and damping coefficient both zero which removed the connection between exercise platform and the wall. For this case, platform displacement remains reasonably small with a peak to peak value of 7.073 mm; however, platform displacement carries an oscillating steady-state error after the excited force stops.

Another simulation is shown in Fig. 9 by adding passive control parameters, spring constant and damping coefficient, to the previous example that damped out the steady-state error in the previous case. For this case, the platform displacement still remains small with a peak-to-peak value of 6.873 mm. A peak-to-peak force, 0.8778 N, is transmitted from the platform

to the wall out of the peak-to-peak input exciter force of 22 N. disturbance forces generated by the exciter. This active and passive controlled VIS reduced 96% of

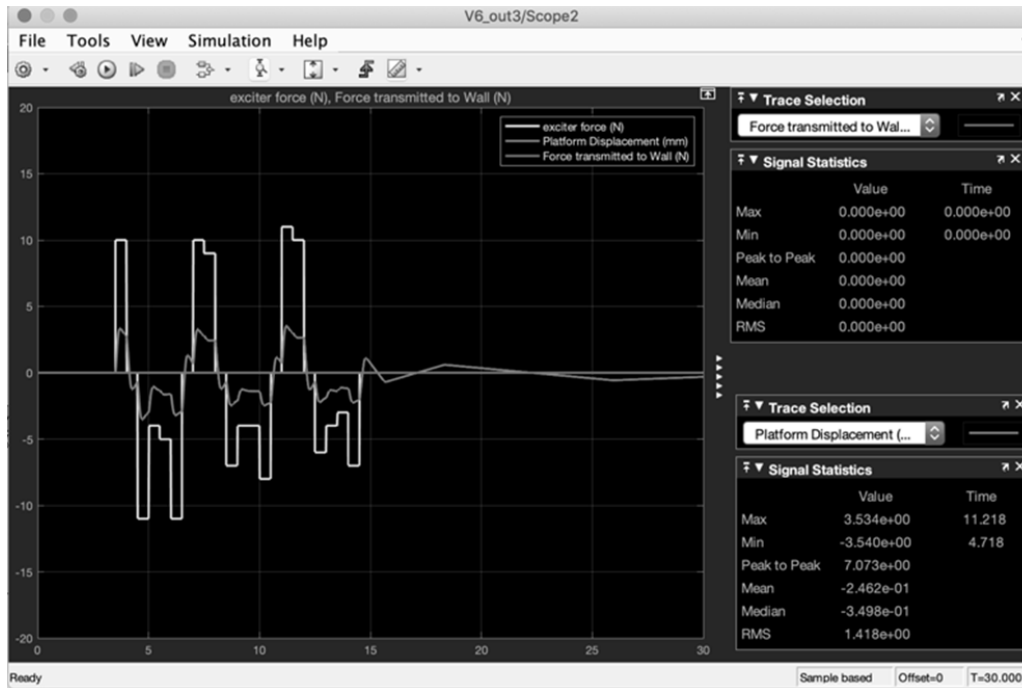


Fig. 8 Simulation Result showing “100%” Vibration Isolation, but with Steady-State Error

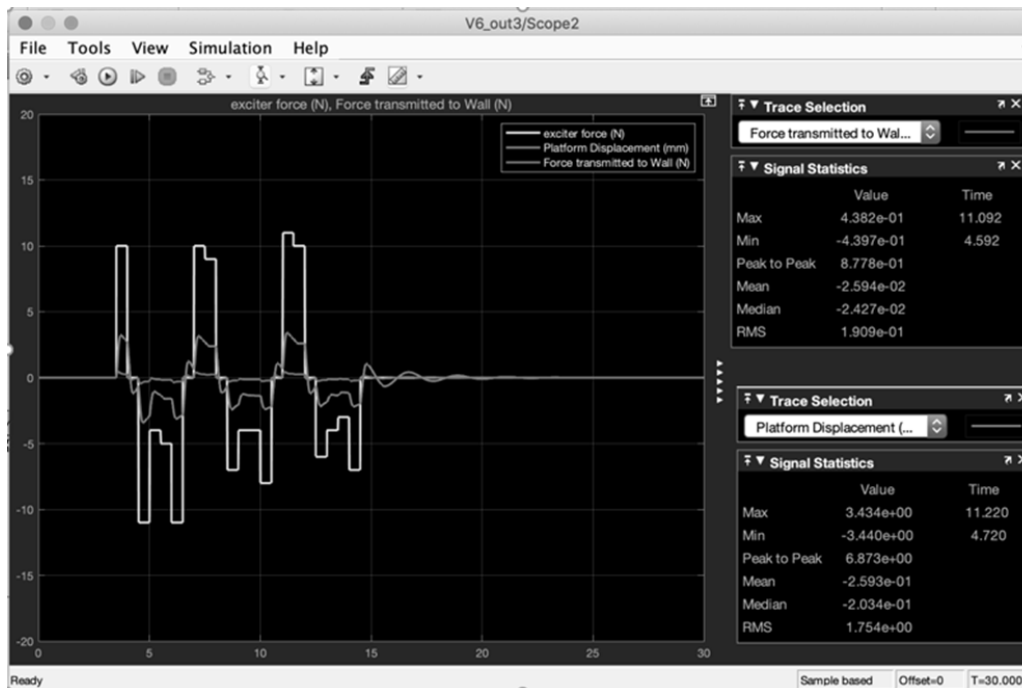


Fig. 9 Simulation Result showing “96%” Vibration Isolation, without Steady-State Error

VI. CONCLUSION

Equations and block diagrams of an active controlled with an optional passive controlled VIS for astronaut’s exercise platform are presented. Computer simulation using Simulink demonstrated promising results that excited forces can be

significantly reduced, even completely eliminated.

The results support the hypothesis of using an active control unit with a counterweight in reducing exercise vibration in a microgravity environment. The future research includes robustness study of the control system to accommodate system

uncertainties and variations of exercise activities.

ACKNOWLEDGMENT

The authors thank Tushar Ghosh, Robert Zehentner, and Daniel Erdberg of CACI, Leslie Quioco and Mike Red at NASA Johnson Space Center (JSC) in Houston, Texas, and many other colleagues working at JSC for the research opportunities, sponsorship and support.

REFERENCES

- [1] J.R. Bagley, K.A. Murach, and S.W. Trappe, "Microgravity-Induced Fiber Type Shift in Human Skeletal Muscle." *Gravitational and Space Biology*, Volume 26(1), pp. 34-40, April 2012.
- [2] A. Hawkey, "The Importance of Exercising in Space," *Interdisciplinary Science Reviews*, 28:2, 130-138, 2003.
- [3] A.J. Calise, J.I. Craig, and B-J Yang, "Adaptive Control for a Microgravity Vibration Isolation System," Final report, NASA Marshall Space Flight Center, Huntsville, AL, March 2006.
- [4] C. Grodsinsky and G. Brown, "Nonintrusive Inertial Vibration Isolation Technology for Microgravity Space Experiments," *Aerospace Research Central*, AIAA-90-0741, August 2012.
- [5] V.C. Nguyen, "A Method to Determine the Optimal Parameters for PID Controller," *International Journal of Engineering and Applied Sciences*, Volume-6, Issue-1, January 2019.
- [6] M. Pabst, M. Darmieder, and R. Theska, "Measuring and Adjusting the Stiffness and Tilt Sensitivity of a Novel 2D Monolithic High Precision Electromagnetic Force Compensated Weighing Cell," *NCSL International Workshop & Symposium*, Cleveland, Ohio, August 2019.
- [7] A.C. Ihedioha and A.M. Anyanwu, "Implementation of an Elevator's Position-Controlled Electric Drive," *International Journal of Trend in Research and Development*, Volume 3(5), September 2016.
- [8] K. Karaman, Y.T. Bekaroglu, M.T. Soylemez, K. Ucak, and G.O. Gunel, "Controlling 3-DOF Helicopter via Fuzzy PID Controller," *International Conference on Electrical and Electronics Engineering*, Bursa, Turkey, November 2015.
- [9] N.L. Segall and P.A. Taylor, "Saturation of Single-Input-Single-Output Controllers Written in Velocity Form: Reset Windup Protection," *Ind. Eng. Chem. Process Des. Dev.*, pp 495-498, 1986.
- [10] MATLAB, written in C/C++ and Java, is a multi-paradigm numerical computing environment and proprietary programming language developed by MathWorks.